PRAMANA
— journal of
physics

Vol. 71, No. 2
August 2008
pp. 283–295

Conformational properties of polymers

A R SINGH[1], D GIRI[2] and S KUMAR[1,*]
[1]Department of Physics, Banaras Hindu University, Varanasi 221 005, India
[2]Department of Applied Physics, Institute of Technology, Banaras Hindu University, Varanasi 221 005, India
[*]Corresponding author. E-mail: yashankit@yahoo.com

Abstract. We discuss exact enumeration technique and its application to polymers and biopolymers. Using this method one can obtain phase diagram in thermodynamic limit. The method works quite well in describing the outcomes of single molecule force spectroscopy results where finite size effects play a crucial role.

Keywords. Polymers and biopolymers; lattice models; exact enumeration; force-induced transitions.

PACS Nos 82.35.Jk; 64.90.+b; 87.14.Gg; 36.20.Ey

1. Introduction

Macromolecules from living organisms vary in their size, shape and function. Some of them are also called 'polymers' because they are made up of long chains of 'monomer' units [1–3]. The monomers can be of different natures. In DNA and RNA they are called nucleotides, and amino acids in proteins. Building blocks of simple artificial polymers can be groups of just a few atoms, e.g., CH_2 in polyethylene. Quite frequently, physicists attempt to simplify complex structures of biopolymers as much as possible. They model polymer chains as threads or necklaces made of beads on a string (modelled by self-avoiding walks), which describes some essential properties of biopolymers [1]. The analogy between critical phenomena (n-vector model of magnetization) and self-avoiding walks (SAWs) in the limit $n \to 0$ benefited polymer physics community in a big way because of the vast knowledge accumulated in the field of critical phenomena [1]. Now there is an intense activity in experiments involving the manipulation of a single biomolecules. This interest has been fueled by the desire to understand the fundamental mechanisms at play in the transcription and replication processes in DNA, elastic, structural and functional properties of proteins and DNA/RNA etc. [4–9]. This became possible because a force ($\sim$pN) may be applied using experimental techniques, such as, atomic force microscopy, optical tweezers, magnetic tweezers etc. [10]. Moreover, these experiments also provide an excellent opportunity to verify theoretical predictions based on the models which are amenable to analytical solution or very

accurate numerical treatments in the framework of statistical mechanics [11–22]. Theoretical and numerical methods which have been used to study force-induced transitions include renormalization group, transfer matrix, Monte Carlo, exact enumeration along with series expansion techniques and generating function technique.

The paper is organized as follows. In §2 and §3 we briefly discuss the various models to describe polymers and method to calculate various observables at the scale of polymer length respectively. In §4 we describe in detail the force-induced desorption of polymer and phase diagram associated with it. The method developed in §4 has been used to study the protein unfolding and DNA unzipping in §5. We mainly describe the key features of these systems in this section. Paper ends with brief conclusion in §6.

2. Model

There are many models of polymers in the literature [1,2] which may be defined in two broad categories: (i) continuum models and (ii) lattice models. Here we shall focus our discussion on lattice models and their basic properties. We illustrate when and how the theoretical descriptions of models fail and further refinements in the model are necessary to explain the experimental observations. A linear polymer chain in a solvent can be modelled by a walk on a lattice in which a step or vertex of the walk represents a monomer. In a random walk model of a polymer, the walk is allowed to cross itself without restriction and the results thus obtained are the same as that of the Gaussian chain [1]. The excluded volume effect can be incorporated in the walk with a constraint that a lattice site cannot be visited more than once. This kind of walk is known as self-avoiding walk (SAW), which simulates a linear polymer chain in a good solvent. A polymer chain in a poor solvent is modelled by self-attracting self-avoiding walks (SASAWs) by including self-attraction among monomers. This model exhibits collapse transition including the existence of θ-point [1]. Various kinds of underlying lattices have been used to study the conformational properties of linear polymer chains. The choice of the lattice depends on the mathematical convenience, nature of the system and the interactions present in the system. As far as universality is concerned, the nature of underlying lattice and the detail of interactions do not matter much and many important properties associated with polymers can be derived, which are in qualitative agreement with the experiments. Sometimes quantitative agreement has also been achieved particularly in determining the critical exponents [1]. Therefore, SAWs with suitable interactions on lattice have been studied extensively in describing the various properties of polymers and biopolymers. In spite of a lot of efforts, an exact solution of problem in 3D has not been possible so far. The model has been solved in 2D exactly and the critical exponents are known [23].

In addition to self-avoidance, one can also introduce additional constraints on the walks, e.g. certain direction(s) is (are) not accessible to the walker and such walks are called directed walks (DWs). To define a directed walk, a preferred direction $\hat{n}$ on the lattice is assigned. Walkers are allowed to take only those steps in the non-negative direction of $\hat{n}$. The directed walk can be seen as a model of polymer that is subjected to some external force in the direction of $\hat{n}$, e.g. flow in which the

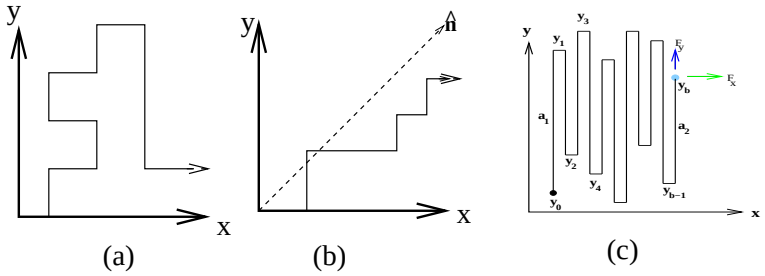

Figure 1. Schematic diagram of SASAW, DW and PDSAW models. A force has been applied at one end (along x-axis) keeping other end fixed. In order to study anisotropy one may apply force along y-axis.

polymer is immersed, or an electric field acting on electrically charged polymers. Depending on the choice of the direction $\hat{n}$, directed walks may be defined in two ways [2,24]:

1. Fully directed walks: If the direction $\hat{n}$ is assigned as shown in figure 1 and walks in the non-negative projection of $\hat{n}$ are not allowed, then such walks are called fully directed walks (FDWs).
2. Partial directed walks: If the direction $\hat{n}$ is assigned, say along the x-axis, then the walks are said to be the partial directed walks (PDSAWs). For example in 2D, the walker can take step in $\pm y$ directions but only in $+x$ direction. This model also exhibits collapse transition in the presence of attractive interaction [25,26].

3. Method: Exact enumeration technique and series analysis

The conformational properties of a polymer chain and phase transition phenomena can be understood if one has the complete information about the partition function of the chain. In the lattice model, the canonical partition function of a polymer chain is calculated [27] by enumerating all possible walks of a given length. The grand canonical partition function can be written as

$$Z(z) = \sum_N C_N z^N. \tag{1}$$

Let C_N be the number of distinct configurations of a chain of N steps and it scales as $\sim\mu^N N^{\gamma-1}$. Here μ and γ are the lattice connective constant and the critical exponent respectively. As the singularity of the partition function is associated with critical phenomena, the partition function defined in eq. (1) will follow $Z(z) \sim (1 - z/z_c)^{-\gamma}$ in the thermodynamic limit. z_c is the critical value of step fugacity for the long chain. In most of the cases, where model is not analytically solvable, one uses numerical techniques [27] to calculate the partition function. Once the partition function is known, other thermodynamic variables can be calculated.

Since in a system of finite size the true phase transition cannot take place, one has to use suitable extrapolation scheme to calculate C_N in the limit $N \to \infty$. For this

purpose, a suitable technique, e.g. ratio method, Pade approximants, differential approximation etc. [27] can be used. In ratio method [27] the approximate value of μ for $N \to \infty$ can be calculated by constructing a Naville table associated with the series. A Naville table can be constructed from the following relation:

$$\mu_N^m = \frac{1}{N-m}[N\mu_N^{m-1} - (N-2m)\mu_{N-2}^{m-1}], \tag{2}$$

where μ_N^0 ($m = 0$ means without approximation) is the value of μ calculated from the relation $\mu_N = \sqrt{\frac{C_{N+2}}{C_N}}$. Here m is the order of the approximation and $m = 1, 2, ...$ corresponds to linear, quadratic,... higher-order approximations of μ_N. Even $m = 0$ (linear extrapolation of small chain data) gives an excellent agreement with known values [27]. In the next section, we will use eq. (2) to calculate μ_N in the limit $N \to \infty$.

4. Application to polymers: Force-induced desorption

We consider SAWs that start from a point on an impenetrable surface and experience a force F in a direction perpendicular to the surface at the other end as shown in figure 2a. The applied force, because of its direction, favours desorption and one expects a critical force (F_c) for desorption. At a given temperature (T) when the applied force F is less than $F_c(T)$ the polymer will be adsorbed, while for $F > F_c(T)$ the polymer will be desorbed. The curve $F_c(T)$, therefore, gives the boundary that separates the desorbed phase from the adsorbed phase in the force–temperature (F, T) plane [28]. Here $C_N(N_s, h)$ corresponds to the number of SAWs of N steps having N_s number of monomers on the surface and h, the height of the end-monomer away from the surface. In this case the partition function may be defined as

$$Z_N(\omega, u) = \sum_{N_s,h} C_N(N_s, h)\omega^{N_s}u^h, \tag{3}$$

where $\omega = e^{-\epsilon_s/k_B T}$ and $u = e^{F/k_B T}$ are the Boltzmann weights for the surface interaction ($\epsilon_s < 0$) and the applied force respectively. In the following, we set the Boltzmann constant $k_B = 1$ and $\epsilon_s = -1$.

For fixed F, we locate the adsorption–desorption transition temperature from the maximum of $(\partial\langle N_s\rangle/\partial(\log\omega))$ (=Fluctuation in adsorbed monomers N_s), where $\langle N_s\rangle = (1/Z_N(\omega, u))\sum_{N_s,h} N_s C_N(N_s, h)\omega^{N_s}u^h$. The force–temperature phase diagram is shown in figure 2. The occurrence of two maxima in a $\partial\langle N_s\rangle/\partial(\log\omega)$ curve gives the signature of re-entrance in 3D, but this feature is absent in 2D [28]. Using the phenomenological argument and the probability distribution analysis, it was shown that the ground state entropy is responsible for the re-entrance which is absent in 2D [28].

It is possible to obtain better estimates of phase boundaries by extrapolating μ for large N. The reduced free energy per monomer in this case is defined as

$$G(\omega, u) = \lim_{N\to\infty} \frac{1}{N} \log Z_N(\omega, u) = \log \mu_N(\omega, u). \tag{4}$$

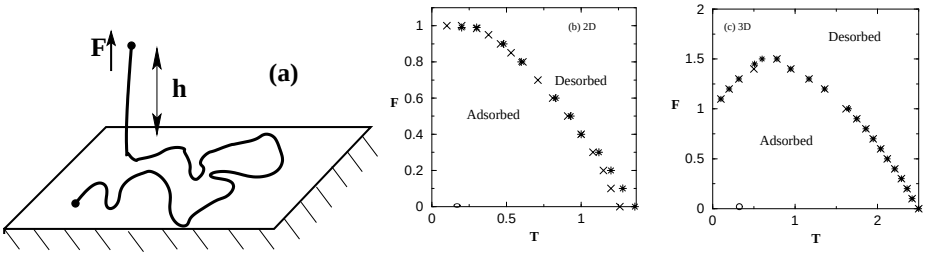

Figure 2. (**a**) Schematic diagram of the polymer chain adsorbed on the surface under the application of external force. The dependence of critical force $F_c(T)$ on T in (**b**) 2D and (**c**) 3D. The star corresponds to results obtained from the extrapolated values of the reduced free energy and cross corresponds to the value obtained from finite size data of a step $N = 20$ (3D) and $N = 31$ (2D) respectively.

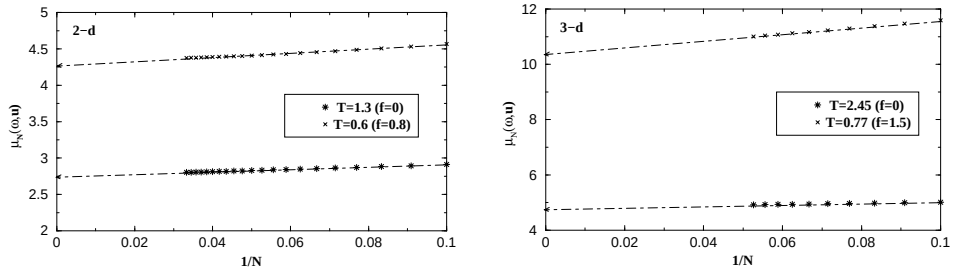

Figure 3. Plot of $\mu_N(\omega, u)$ vs. $1/N$ for 2D and 3D. A linear extrapolation gives the value at $N = \infty$.

$\mu_N(\omega, u)$ can be estimated from the partition functions found from the data of exact enumerations for finite N by extrapolating to large N. The value of $\mu_N(\omega, u)$ as a function of $1/N$ for different values of F and T for 2D and 3D is shown in figure 3. The extrapolated value of $\mu_N(\omega, u)$ for $(1/N) \to 0$ has been used in eq. (3) to calculate the reduced free energy per monomer.

5. Application to biopolymers

The method developed in the previous section may be applied to study the force-induced transitions in biopolymers. In the following we will discuss two problems, namely protein unfolding and DNA unzipping.

5.1 *Protein unfolding*

The linear amino acid sequence of a polypeptide chain which encodes the information required to fold to a native state was first shown by Anfinsen [29]. The ability to predict not only the native structure from a linear amino acid sequence, but also

the pathways along which the reaction proceeds is known as the protein folding. This process of folding fascinated many including physicists, chemists, biologists, mathematicians and computer scientists for several decades. The mechanism by which a polypeptide chain is able to fold rapidly to the native state, despite the very large number of conformations that exist for the chain is known as Levinthal paradox [30]. The paradox was solved by the realization that proteins fold through parallel processes leading to the idea that the free energy surface of a folding peptide is funnel shaped. In order to have better understanding of the energy landscape, attempts have been now made to apply the force in pN range, most commonly using optical tweezers, atomic force microscopes, glass microneedle etc. [7–9,31].

The force-extension curve obtained in experiments for a protein like titin shows the saw-tooth-like structure which gives important information about the elastic and structural properties of titin [7,31]. For theoretical understanding, we model such molecule by a homo semi-flexible polymer chain by considering SASAW's on a square lattice with a force applied at one end [32,33] as shown in figure 1. Stiffness in chain can be introduced by associating a positive energy with each bending. Inclusion of bending energy and replacing surface interaction by monomer–monomer interaction in the partition function defined by eq. (3) give the following key features of the system:

- For zero force, the phase diagram consists of three distinct phases: (i) an open coil state, (ii) a globule state at low stiffness and (iii) a frozen or folded state at low temperature and large stiffness similar to β-sheet which is close to structure of the protein titin found in muscle [32].
- For flexible polymer chain, the force–temperature diagram (figure 4a) exhibits the re-entrance behaviour at low temperature [32,33].
- Force–extension curve shows the presence of intermediate states (figure 4b) as seen in recent unfolding experiments [32–36]. The multi-step character washes out as temperature increases (figure 4b).
- The extension of length up to 55 allowed us to obtain a new line in between extended state and stretched state which is induced by the force [33]. In contrast to the lower phase boundary, where the force decreases with temperature, the upper boundary shows that force increases with temperature (figure 4a). In a recent paper, we showed that this is indeed a cross-over effect [37].
- Experimental set-up such as atomic force microscope mostly used in such study works in constant distance ensemble (CDE). Inclusion of stiffness in CDE shows the saw-tooth-like behaviour in force–distance (figure 4c) curve as seen in experiments [33].
- Using the PDSAWs model (figure 1c), it was shown that the collapse transition is of the second order for a polymer with exactly zero bending stiffness [25]. However, finite bending shows that it is of the first order. Therefore, bending energies have a dramatic effect on the cooperativity of the 2D globule-coil transition. This has been substantiated by extensive Monte Carlo simulations [25].
- Single molecule manipulation techniques reveal that the mechanical resistance of a protein depends on the direction of the applied force [38–40]. This is

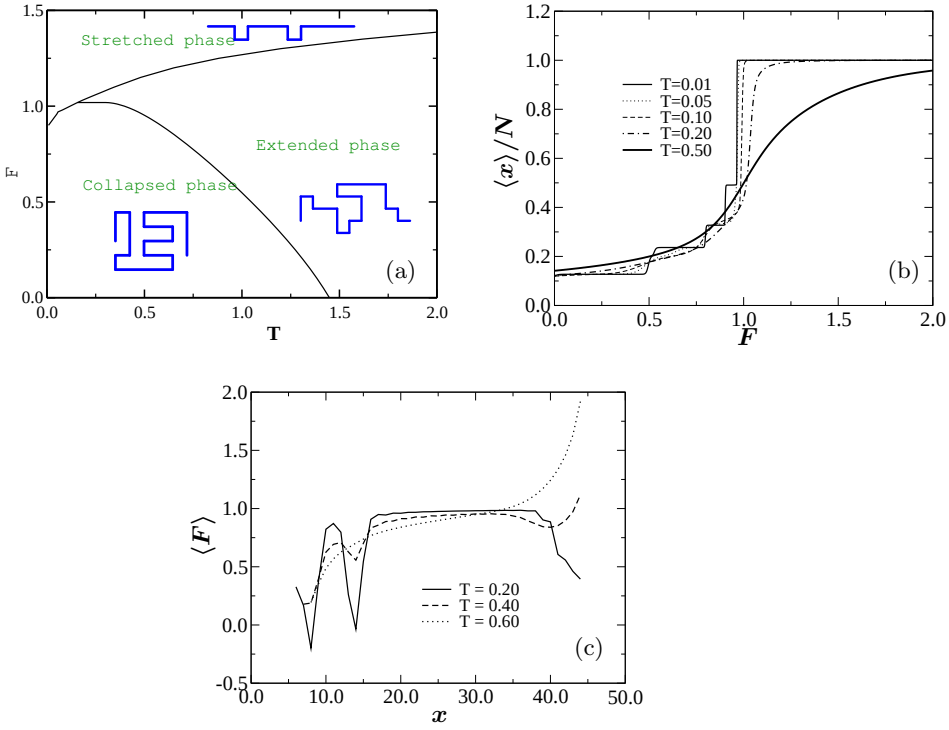

Figure 4. (**a**) The force–temperature phase diagram for flexible polymer chain. Lower boundary shows that temperature decreases with force while upper line shows that temperature increases with force. (**b**) Plot of $\langle x\rangle/N$ vs. F at different temperatures for length $N = 55$. (**c**) Plot of $\langle F\rangle$ vs. x at different T for $N = 55$ in CDE.

because all proteins are highly anisotropic in shape and interactions. One therefore expects that their mechanical properties, e.g., compressibility, Young's modulus, etc. depend on the direction and orientation. We have studied the molecular origin of protein resistance to unfolding [26,41] by considering a PDSAWs (inherently anisotropic) model of polymer. The analytical solution of the model [41] shows that a change in the pulling direction gives rise to different phase diagrams even in the thermodynamic limit. At a given temperature, pulling force along y-direction is more than along the x-direction. This is evident from the F–T phase diagram shown in figure 5a.

- Change in pulling direction gives rise to emergence of new intermediate states as shown in figures 5b and 5c.
- It was shown that when a chain is being pulled along the x-direction (figure 6b) the nature of the transition is akin to unzipping (smooth plateau in F–x curve shown in figure 6c), but when force is applied along the y-direction (figure 6a) the transition is akin to shearing (saw-tooth-like behaviour as shown in figure 6d).

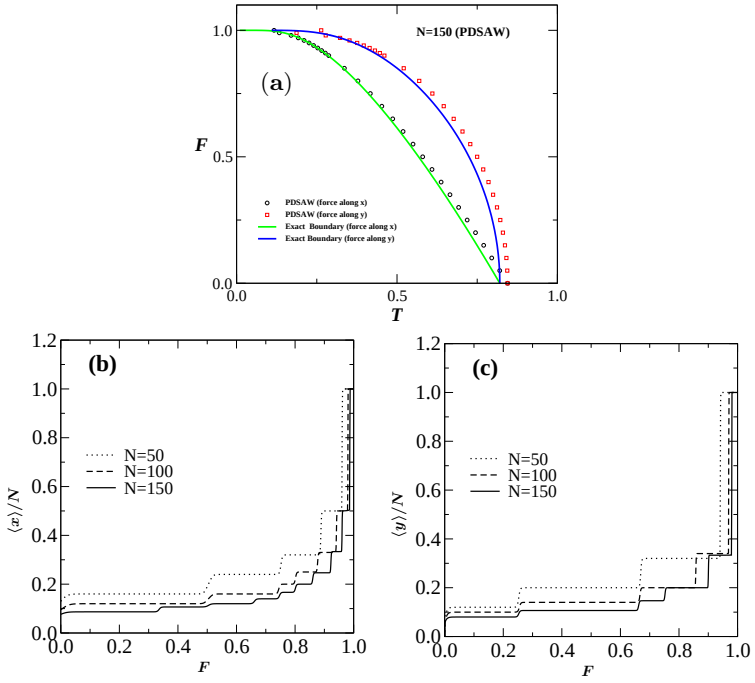

Figure 5. (**a**) The force–temperature phase diagrams for PDSAW. (**b**) and (**c**) Plots of the average extension $\langle x\rangle/N$ ($\langle y\rangle/N$) vs. the applied force F for chain lengths $N = 150$, 100 and 50 at fixed temperature $T = 0.01$ with the force along the x-direction (y-direction). The emergence of intermediate states when a force is applied along x-axis is evident from the plot.

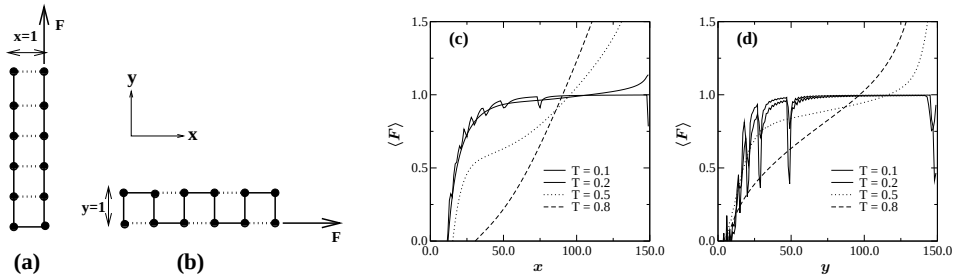

Figure 6. Schematic representation of two cases (having $N/2$ contacts and $N/2$ extension) where a force is applied along (**a**) the y-direction, (**b**) the x-direction. (**c**) and (**d**) Plot of the average force $\langle F\rangle$ vs. the elongation at different temperatures T for chain length $N = 150$. The marked difference due to a change in pulling direction is clear from these plots.

5.2 *DNA unzipping*

DNA is a heteropolymeric molecule consisting of residues (nucleotides) of four types: cytosine (C), guanine (G), adenine (A) and thymine (T). The bases are capable of

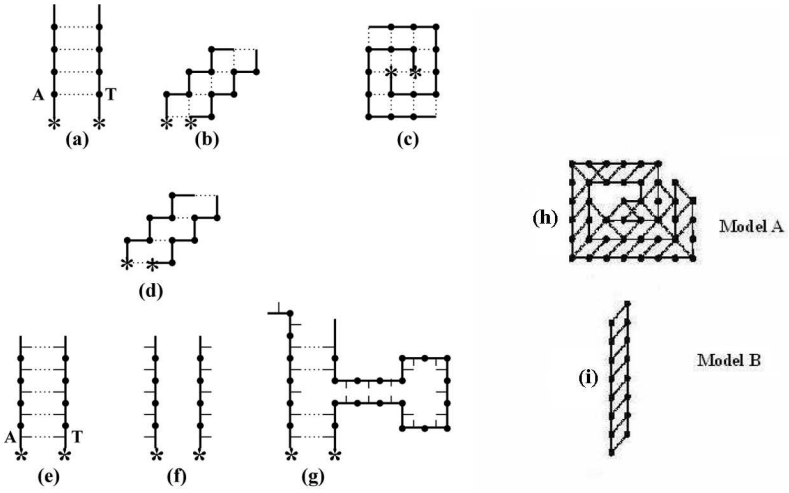

Figure 7. Figures (**a**)–(**c**) represent the possible conformations of models A. Figures (**a**) & (**d**) are possible conformations of model B. Figure (**c**) corresponds to the ground state of model A, while figure (**a**) corresponds to the ground state of model B. Figures (**e,f,g**) represent model C where bases are on the links of the strands with short stubs representing orientation. (**e**) the completely zipped state, (**f**) a nonpairing configuration, and (**g**) a partial bound configuration with hairpin loop. In all cases dotted lines show the attractive interactions. (**h**) & (**i**) Possible ground states of models A and B with diagonal interactions.

forming hydrogen bonds among them, but in a selective way. A can couple with T and G to C. The A-T base pair involves the formation of two hydrogen bonds while C-G contains three hydrogen bonds. The strength of a hydrogen bond typically lies between 2 and 4 kcal/mol. With the rise of temperature or change of the pH of the solvent, base pairs may open and bubble forms. At a certain temperature, the number of intact base pairs drop abruptly and two strands are separated. This process is known as thermal denaturation of DNA or DNA melting [42]. The temperature at which half of the total base pairs are open is termed as melting temperature, which lies between 80 and 100°C. It took almost four decades to realize that unzipping of double stranded DNA (dsDNA) may be achieved with a force applied solely at one end instead of varying the temperature or pH of the solvent [11–13,43,44]. This elucidated a better understanding of the mechanism involved in crucial processes like transcription and replication [43–47].

Theoretical modelling of dsDNA [20–22] may be done in two ways: (1) any monomer of one strand can interact with any monomer of the other strand (we call it as model A as shown in figures (7a–7c) and (2) a monomer i of one strand can only interact with the ith monomer of the other strand (model B shown in figures 7a and 7d). This second model is similar to the model of DNA studied earlier by Poland and Scheraga (PS) [42]. PS model does not take into account the directional nature of the hydrogen bond and underestimate the entropy by restricting the formation of hydrogen bonds between 'non-native' pair of nearest-neighbouring bases. The

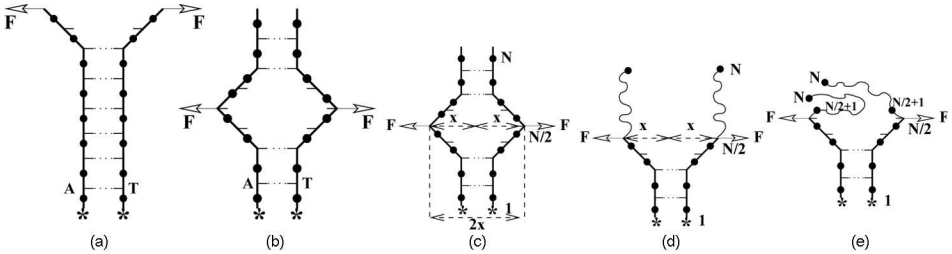

Figure 8. Schematic representation of DNA when a force is applied at (**a**) one end, (**b**) applied at the interior of the two strands; (**c–e**) Schematic diagram for the mid-case showing different conformations keeping $2x$ ($\leq N^{\nu}$, where ν is the end-to-end distance exponent) distance constant. For model B, (**d**) and (**e**) has same weight while for model C, (**e**) has more weight than (**d**).

importance of bubble formation during thermal melting has been recognized but no attempt has been made so far to experimentally explore the phase diagram of unzipping DNA when a force is applied to the interior of the chain.

We consider two linear polymer chains made up of say adenine (A) and its complementary thymine (T) which are mutually-attracting-self-avoiding walks (MASAWs) on a square lattice as shown in figures 7a–7d. There is another more realistic model of dsDNA where directional nature has been taken into account [21,22]. We call it model C, the details of which are shown in figures 7e–7g. We consider two cases: (I) a force is applied at the end (figure 8a) of the chain (analogous to replication) and (II) a force is applied at the middle (figure 8b) of the chain (analogous to transcription). The model may be generalized to any dimensions [48], but for computational limitations, we consider it on square lattice only. The modified partition function for this system may be written as

$$Z_N(\omega, u) = \sum_{m,x} C(m, x) x_1^N x_2^N \omega^m u^x. \tag{5}$$

Here x_1 and x_2 are the fugacities associated with each step of the two self-avoiding walks representing the two strands respectively. ω is the Boltzmann weight associated with the binding energy of each base pair and m is the total number of intact base pairs in the chain. Semi-microscopic variation in models gives rise different behaviour [20–22] which are listed below:

- Model A which is basically two interacting polymers exhibits two zero force thermal phase transitions [20,22]. First system goes from the collapsed state to helix-like state with the rise of temperature. Further increase in temperature leads system to the segregated state. The collapse-like state may be useful in understanding the packing of DNA in the cell. Model A also shows the existence of a force-induced triple point in F–T phase diagram.
- In order to study the role of bubble formation during DNA unzipping, a force is applied to the interior of the chain. The melting profile and force–extension curves of models B and C remain almost the same for end case [21,22], but differ for the mid-case. Non-native interaction in model C shows the existence

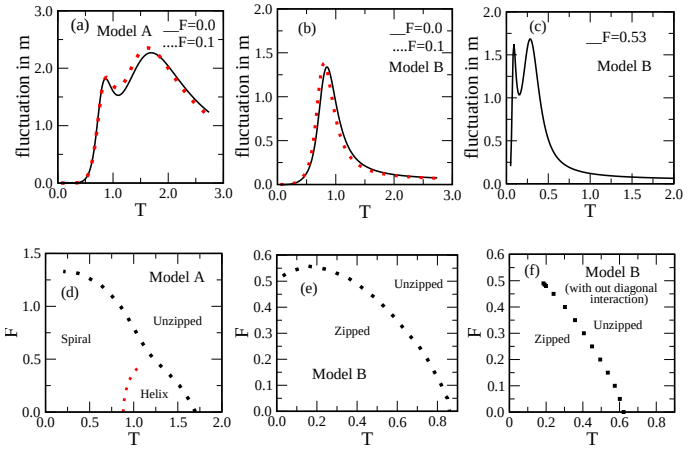

Figure 9. Plots of fluctuation in m vs. T for $F = 0.0, 0.1$ with diagonal interaction for (**a**) model A, (**b**) model B. (**c**) shows the fluctuation in m for higher value of force. (**d**) and (**e**) Force–temperature phase diagram for models A and B. For the sake of comparison, we have also shown in (**f**) the phase diagram of model B with nearest-neighbour interaction where re-entrance behaviour was found to be absent [20,22].

of an 'eye-phase' even at higher temperatures [21]. This has been established by observing oscillations in the probability distribution curve. The important outcome of our studies is that when a force is applied in the middle, half of the chain undergoes unzipping kind of transition (figures 8c–e) while the other half goes to shearing (slippage) kind of transition [21,22] (figure 8).

- It is pertinent to mention that collapse to helix transition remains absent in models B and C as evident from figure 9b. Moreover, models B and C have no re-entrance in F–T phase diagram (figure 9e). This is because of the lattice constraint which inhibits the ground state entropy of the zipped state. The semi-microscopic change in the interaction may give rise the re-entrance behaviour. Instead of taking the formation of base pair as nearest neighbour, if one takes base pairing among the diagonal nearest neighbour, one may observe the re-entrance in force–temperature plane. Because the ground state entropy for such a system is sufficiently large, the fluctuation in base pairing indeed gives two peaks which is the signature of the re-entrance as shown in figure 9c. The modified force–temperature diagram with diagonal interaction [49] shows the re-entrance behaviour as shown in figure 9e. The other features remain the same as of nearest-neighbour interaction.

6. Conclusion

We have briefly discussed the lattice models for polymers and biopolymers. As we have exact information about the density of states, the exact enumeration technique

provides better understanding of force-induced transitions in biomolecules. The existence of triple point, effects of eye-phase, role of pulling directions, effects of temperature in constant force ensemble etc. are some of the issues which require additional numerical efforts to understand force-induced transitions in biomolecules.

Acknowledgments

The authors thank the University Grants Commission, New Delhi and Department of Science and Technology, New Delhi for financial support.

References

[1] P G de Gennes, *Scaling concepts in polymer physics* (Cornell Univ. Press, Ithaca, 1979)
S Kumar and Y Singh, *Phys. Rev.* **A42**, 7151 (1990)
[2] C Vanderzande, *Lattice models of polymers* (Cambridge Univ. Press, Cambridge, 1998) and references therein
[3] *Statistics of linear polymers in disordered media* edited by B K Chakrabarti (Elsevier, Amsterdam, 2005)
[4] M Carrion-Vazquez, A F Oberhauser and T E Fisher, *Prog. Biophys. Mol. Bio.* **74**, 63 (2000)
A Engel, H E Gaub and D J Muller, *Curr. Biol.* **9**, R133 (1999)
[5] U Bockelmann, *Curr. Opin. Struc. Biol.* **14**, 368 (2004)
[6] P Cluzel, A Lebrun, R Heller, R Lavery, J-L Viovy, D Chatenay and F Caron, *Science* **271**, 792 (1996)
[7] M Rief, M Gautel, F Oesterhelt, J M Fernandez and H E Gaub, *Science* **276**, 1109 (1997)
[8] M S Z Kellermayer, S B Smith, H L Granzier and C Bustamante, *Science* **276**, 1112 (1997)
C Bustamante, J Liphardt and F Ritort, *Physics Today* **58**, 43 (2005)
[9] L Tskhovrebova, J Trinick, J A Sleep and R M Simmons, *Nature (London)* **387**, 308 (1997)
[10] C Bustamante, Y R Chemla, N R Forde and D Izhaky, *Annu. Rev. Biochem.* **73**, 705 (2004)
[11] S M Bhattacharjee, *J. Phys.* **A33**, L423 (2000), cond-mat/9912297
[12] K Sebastian, *Phys. Rev.* **E62**, 1128 (2000)
[13] D K Lubensky and D R Nelson, *Phys. Rev. Lett.* **85**, 1572 (2000)
[14] D Marenduzzo, A Trovato and A Maritan, *Phys. Rev.* **E64**, 031901 (2001)
[15] D Marenduzzo, S M Bhattacharjee, A Maritan, E Orlandini and F Seno, *Phys. Rev. Lett.* **88**, 028102 (2002)
[16] R Kapri, S M Bhattacharjee and F Seno, *Phys. Rev. Lett.* **93**, 248102 (2004)
R Kapri and S M Bhattacharjee, cond-mat/0511531
[17] Puri-Man Lam *et al*, *Biopolymers* **73**, 293 (2004)
[18] Jeff Z Y Chen, *Phys. Rev.* **E66**, 031912 (2002)
[19] E Orlandini *et al*, *J. Phys.* **A34**, L751 (2001)
[20] S Kumar, D Giri and S M Bhattacharjee, *Phys. Rev.* **E71**, 51804 (2005)
[21] D Giri and S Kumar, *Phys. Rev.* **E73**, 050903(R) (2006)

[22] S Kumar and D Giri, *J. Chem. Phys.* **125**, 044905 (2006)
[23] B Duplantier and H Saleur, *Phys. Rev. Lett.* **57**, 3179 (1986)
[24] P K Mishra, S Kumar and Y Singh, *Physica* **A323**, 453 (2003)
[25] H Zhou, J Zhou, Z-C O-Yang and S Kumar, *Phys. Rev. Lett.* **97**, 158302 (2006)
[26] S Kumar and D Giri, *Phys. Rev. Lett.* **98**, 048101 (2007)
[27] A J Guttmann, *Phase transitions and critical phenomena* edited by C Domb and J L Lebowitz (Academic Press, New York, 1989) Vol. 13
[28] P K Mishra, S Kumar and Y Singh, *Europhys. Lett.* **69**, 102 (2005)
[29] C Anfinsen, *Biochem. J.* **128**, 737 (1972)
[30] C Levinthal, *J. Chim. Phys.* **65**, 44 (1968)
[31] M Carrion-Vazquez *et al*, *Proc. Natl Acad. Sci.* **96**, 3694 (1999)
[32] S Kumar and D Giri, *Phys. Rev.* **E72**, 052901 (2005)
[33] S Kumar *et al*, *Phys. Rev. Lett.* **98**, 128101 (2007)
[34] D Marenduzzo *et al*, *Phys. Rev. Lett.* **90**, 088301 (2003)
[35] B J Haupt, T J Senden and E M Sevick, *Langmuir* **18**, 2174 (2002)
[36] A S Lemak, J R Lepock and J Z Y Chen, *Phys. Rev.* **E67**, 031910 (2003)
A S Lemak, J R Lepock and J Z Y Chen, *Proteins: Structures, function and genetics* **51**, 224 (2003)
[37] S Kumar and G Mishra, *Phys. Rev.* **E78**, 011907 (2008)
[38] G Yang *et al*, *Proc. Natl. Acad. Sci.* **97**, 139 (2000)
[39] H Dietz and M Rief, *Proc. Natl. Acad. Sci.* **103**, 1244 (2006)
[40] D Brockwell *et al*, *Nature Struc. Biol.* **10**, 731 (2003)
[41] R Rajesh, D Giri, I Jensen and S Kumar, *Phys. Rev.* **E78(2)**, (in press)
[42] D Poland and H A Scheraga, *J. Chem. Phys.* **45**, 1456 (1966); *ibid.* **45**, 1464 (1966), *Theory of helix-coil transitions in biopolymers* (Academic, New York, 1970)
S Kumar and Y Singh, *J. Phys. A: Math. Gen.* **26**, L987 (1993)
[43] U Bockelmann, B Essevaz-Roulet and F Heslot, *Phys. Rev. Lett.* **79**, 4489 (1997)
[44] U Bockelmann, B Essevaz-Roulet and F Heslot, *Phys. Rev.* **E58**, 2386 (1998)
[45] G U Lee, L A Chrisey and R J Cotton, *Science* **266**, 771 (1994)
[46] C Danilowicz *et al*, *Phys. Rev. Lett.* **93**, 078101 (2004)
[47] C Danilowiicz *et al*, *Proc. Natl. Acad. Sci.* **100**, 1694 (2003)
[48] S Kumar, D Giri and Y Singh, *Europhys. Lett.* **70**, 15 (2005)
[49] A R Singh, D Giri and S Kumar, Preprint (2008)